ELSEVIER

Nuclear Instruments and Methods in Physics Research B 141 (1998) 123–132

NIM B
Beam Interactions with Materials & Atoms

Amorphization of SiC under ion and neutron irradiation

L.L. Snead *, S.J. Zinkle, J.C. Hay, M.C. Osborne

Metals and Ceramics Division, Oak Ridge National Lab., Bldg., 4508; MS6087, Oak Ridge, TN 37831-6087, USA

Abstract

This paper presents results on the microstructure and physical properties of SiC amorphized by both ion and neutron irradiation. Specifically, 0.56 MeV Si ions have been implanted in single crystal 6H–SiC from ambient through >200°C and the critical threshold for amorphization was measured as a function of the irradiation temperature. From a high resolution transmission electron microscopy (HRTEM) study of the crystalline to amorphous transition region in these materials, elongated pockets of amorphous material oriented parallel to the free surface are observed. Single crystal 6H–SiC and hot pressed and sintered 6H and 3C SiC were neutron irradiated at approximately 70°C to a dose of ~2.56 dpa causing complete amorphization. Property changes resulting from the crystal to amorphous transition in SiC include a density decrease of 10.8%, a hardness decrease from 38.7 to 21.0 GPa, and a decrease in elastic modulus from 528 to 292 GPa. Recrystallization of the amorphized, single crystal 6H–SiC appears to occur in two stages. In the temperature range of ~800–1000°C, crystallites nucleate and slowly grow. In the temperature range of 1125–1150°C spontaneous nucleation and rapid growth of crystallites occur. It is further noted that amorphized 6H (alpha) SiC recrystallizes to highly faulted fcc (beta) SiC. © 1998 Published by Elsevier Science B.V. All rights reserved.

PACS: 61.80.Jh; 61.82.Ms
Keywords: SiC; Amorphization; Ion bombardment

1. Introduction

Silicon carbide possesses a range of interesting physical properties which make it an attractive material for applications ranging from heat engines to electronic devices to nuclear systems. For the latter two applications, the effects of displacive radiation on the structure and ultimate material performance are key issues. In particular, for the processing of SiC devices, ambient temperature implantation of dopant ions and their effects on microstructure are of importance while the swelling and mechanical properties of SiC subjected to displacive neutron irradiation are important in nuclear applications. In such irradiations the most dramatic material and microstructural changes occur during irradiation at low temperatures. Specifically, at temperatures under 100°C volumetric swelling due to point defect induced strain has been seen to reach 3% for neutron irradiation doses of ~0.1–0.5 [1,2]. At these low temperatures,

* Corresponding author. Tel.: 423 574 9942; fax: 423 576 8424; e-mail: z2n@ornl.gov.

0168-583X/98/$19.00 © 1998 Published by Elsevier Science B.V. All rights reserved.
PII S0168-583X(98)00085-8

amorphization of the SiC is also possible, which would lead to a substantial volumetric expansion of ~15%, [3–5] along with decreases in mechanical properties such as hardness and modulus [3,4,6]. Specifically, Snead et al. [6] found that the elastic modulus for chemically vapor infiltrated SiC decreased from 400 GPa in the unimplanted region following 3 MeV carbon ion irradiation, to ~275 GPa in the amorphized region. Likewise, the hardness was seen to decrease from 41 GPa to 32 GPa. Similar behavior has been recently reported by other authors [5] for ion irradiated SiC.

Numerous studies [7–14] have shown that SiC becomes amorphous during ion-beam irradiation at temperatures between 77 K and room temperature for damage levels of approximately 0.1–0.5 dpa. The majority of studies relating to SiC amorphization have utilized low-energy (<1 MeV) ion-beams [9–14], with a few researchers studying the amorphization threshold using high energy electrons [15–18]. These electron and ion irradiation studies have typically been carried out at temperatures between liquid nitrogen (77 K) and 470 K.

To date there has been no demonstration of neutron induced amorphization of SiC, although it is worth noting that there is a lack of low temperature, high dose neutron irradiation data. Amorphization was not observed in SiC irradiated with fission neutrons (damage rate $\sim 10^{-7}$ dpa/s) at ~420 K to damage levels in excess of 1 dpa [19]. In fact, there has been no demonstration of amorphization caused by fast neutron displacements in any ceramic material. While amorphization has been demonstrated for neutron irradiated quartz [20–22], the transition is due to radiolysis rather than due to displaced atoms. Graphite has also been claimed to amorphize under neutron irradiation [23,24] at dose and temperatures <1 dpa and 200°C, though, as pointed out by Kelly [25], the Raman spectra used as an indication for amorphization is consistent with the formation of in-plane edge dislocation dipoles. Another convincing piece of evidence against the neutron amorphization of graphite as quoted by previous authors is that the dimensional change continues to behave anisotropically above the dose levels of apparent amorphization [25].

In the past 10 years there has been a growing interest in the effect of irradiation temperature on the amorphization of silicon carbide. Specifically, Kinoshita [15] and Matsunaga [18] used 1 MeV electron irradiation to measure the damage threshold for amorphization from liquid nitrogen temperature to room temperature. Inui [16,17,26] has used 2 MeV TEM electrons and Weber [5,27–30] has used a 1.5 MeV Xe beam in conjunction with (non-damaging) TEM to perform in situ amorphization studies. In all cases the critical threshold for amorphization was measured as a function of temperature. It was observed that there is a temperature-independent amorphization dose at low temperatures followed by a temperature above which the damage level required to amorphize SiC increases rapidly. In each case an apparent asymptotic increase in the critical dose for amorphization occurred, yielding a critical temperature above which amorphization is apparently not possible. The critical temperatures above which amorphization does not occur has been reported to range between 290 K and 340 K for electrons, [16,17,26] ~420 K for Si ions [31] and ~490 K for Xe ions [5] with similar damage rates of $\sim 1 \times 10^{-3}$ dpa/s. It is noted that both Weber et al. [5,28] and Matsunaga's [18] work did not observe a significant difference in amorphization threshold between α and β SiC, whereas Inui reported a threshold temperature ~50 K lower for α-SiC [17]. The β-SiC used in the study by Inui and coworkers was heavily faulted, which may have influenced the amorphization behavior.

2. Experimental

The materials chosen for this study were Cree Systems single crystal 6-H α-SiC, Cercom hot pressed β-SiC, and Carborundum sintered α-SiC (Hexoloy). Two ion beams were selected for implantation in orientations both normal and parallel to the basal plane. Specifically, both 3.0 MeV C and 0.56 MeV Si ions were implanted as single beams. The silicon beam was produced in the NV-500 accelerator at the SMAC user facility at ORNL, whereas the carbon ion beam was produced in the Triple Ion Beam Facility at ORNL.

In both facilities, samples were heat-sinked to a thermalizer block and temperatures measured using thermocouples either in contact with the thermalizer block or a backing to which the block was clamped. Typical ion beam fluxes were 7.1×10^{11}–2.6×10^{12} ion/cm^{2}s, producing peak displacement damage rates of $\sim 0.2 \times 10^{-3}$–1×10^{-3} dpa/s assuming a sublattice-averaged displacement energy of 40 eV. Cross-sectional transmission electron microscopy (TEM) was performed on all samples. The determination of amorphization was made by bright and dark field imaging and the presence of spot-free, diffuse diffraction patterns. The width of the buried amorphous layer was measured and compared with the TRIM-92 [32] code to determine the critical dose for amorphization. As the fluence was increased from the values used in the calculation the entire range of materials became amorphous. A benefit to the choice of relatively high ion beam energies is that the beginning of the buried amorphous band (used in the threshold calculation) was not in the ion implanted region of the sample. All damage calculations were obtained assuming a sublattice-averaged threshold displacement energy of 40 eV. High resolution TEM was performed with a JEOL 4000 EX microscope, while conventional microscopy was performed using a Philips CM-12 microscope. Samples prepared for microscopy were mechanically thinned and ion milled with argon ions at 6 keV and 15° using a liquid-nitrogen-cooled stage during milling. After foil perforation, the specimens were milled at 3 keV, 9° for 10 min at ambient temperature to reduce surface amorphization associated with argon implantation. X-ray diffraction was carried out using a Rigaku rotating anode diffractometer.

Three-millimeter diameter discs of Carborundum sintered α-SiC (Hexoloy) and Cercom hot pressed β-SiC were irradiated in the target region of the High Flux Isotope Reactor in a thin-walled aluminum capsule that was in direct contact with the reactor coolant water, producing a specimen irradiation temperature of ~70°C. A second capsule containing Cree single crystal 6H (alpha) SiC was irradiated such that the samples were in direct contact with the ~60°C coolant water. The fast neutron ($E > 0.1$ MeV) fluence was $\sim 1.5 \times 10^{26}$ m^{-2} corresponding to a displacement level of ~15 dpa for the sintered α-SiC and the hot pressed β-SiC at a damage rate of $\sim 1 \times 10^{-6}$ dpa/s. The single crystal α-SiC was irradiated to a dose of ~2.6 dpa.

Specimen densities were obtained using density gradient columns mixtures of tetrabromethane-methylene iodide or ethylene bromide-bromoform for the unirradiated and irradiated samples, respectively. The accuracy of the measurement was better than 0.001 g/cc and was found to be reproducible in repeated measurements and consistent for duplicate samples. Hardness and elastic modulus were found using a Nanoindentor™-II with a peak loading of 30 mN. All indentations were performed using a constant loading rate of 1.5 mN/s to a peak load of 30 mN.

3. Results and discussion

3.1. Amorphization under charged particle irradiation

The temperature dependence for amorphization of SiC has been measured by several researchers [5,15–18,26,28–30] either by using irradiation followed by TEM or Rutherford Backscattering (RBS) observation, or by in situ techniques. For the in situ approach, an irradiating beam is passed through, or partially through, a thin section of material with real-time observation of the microstructural evolution using TEM. Fig. 1 compares the conventional (ex situ) data from the Si ion irradiations of this study with the in situ data from Inui [17] and Weber, all of which were obtained at a damage rate near 1×10^{-3} dpa/s. All of the data in Fig. 5 have been plotted assuming an average displacement energy of 40 eV. Inui [16,17,26] used 2 MeV electrons to both damage and image the samples. Weber [5,28–31] used a 1.5 MeV Xe beam in conjunction with TEM. In these examples Inui found the amorphization dose threshold below room temperature to be approximately 1 dpa for α-SiC [17] and about 0.5 dpa for highly faulted β-SiC [16]. Weber [28] found the amorphization threshold near room temperature to be about 0.2 dpa for 1.5 MeV Xe ions.

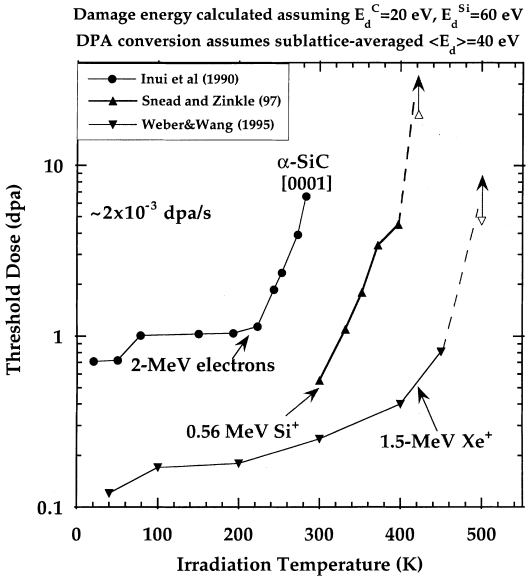

Fig. 1. Temperature dependence on the critical amorphization threshold for Si ion SiC.

The results of Fig. 1 raise interesting questions regarding the mechanism for amorphization in SiC. Because amorphization has occurred under electron irradiation it is apparent that the SiC crystal, in the cubic or hexagonal form, can be made amorphous by simple defect accumulation alone. The Xe ions, which transfer much higher energies to the lattice atoms than the electrons (or the Si ions), are apparently capable of amorphizing SiC to a much higher temperature than electrons at the same damage rate. While the Xe ions will cause relatively large cascades compared to Si ions, no cascades can form for the low energy transfer electron irradiations. This supports the possibility of amorphization beginning within cascade structures which would also explain why the Xe ions produce amorphization to a higher temperature than the Si ions. Alternatively, it is possible that the heavier Xe ions simply create a higher concentration of "stable" interstitials than the Si ions or electrons on a dpa-normalized basis, thus driving the temperature threshold higher. The qualitative aspects of Fig. 1 can be explained if one considers that the amorphization in SiC is due to free energy increases associated with point defect accumulation and chemical disordering [33]. Since the amount of chemical disordering per dpa increases with increasing primary knock-on atom (PKA) energy, less displacement damage is required to produce amorphization with heavy ions compared to electrons at all temperatures.

A potential problem in comparing the amorphization threshold data sets presented in Fig. 1 is whether in situ measurements such as that used by Inui and Weber [5,16,17,26,28–30,34] can be directly compared with the ex situ measurements of the present study. In other words, are there technique-dependent effects occurring for one or both types of amorphization measurements. One example of an experimental artifact is demonstrated by observing a series of high resolution TEM images from the Si implanted, single crystal β-SiC. In general, there is a fairly rapid transition from crystalline material into the amorphous band. As expected from the damage gradient of the ion profile, [7] this transition region is wider at the near-surface side of the amorphization band compared to the end of the band (larger gradient in damage.) Fig. 2 shows a HRTEM bright field image of the crystalline to amorphous transition region at the end of the amorphous band for a 6H–SiC sample irradiated with Si ions normal to the *c*-axis at 60°C. Of particular interest in this micrograph are the shape and orientation of the amorphous areas, which appear to form as island structures with the major radii aligned parallel to the surface of the specimen. This phenomenon was observed in all amorphized specimens studied at both the beginning and end of the amorphized region from 60°C to 125°C for the Si ion irradiated specimens. These anisotropic amorphous structures occur when the beam is injected normal to the *c*-axis (as in Fig. 2) or parallel to the *c*-axis and therefore is not a crystallographic orientation phenomenon. Fig. 3 shows another bright field micrograph illustrating that the formation of these islands occurs on a nanometer scale, eventually growing and linking with other islands. A previous study [7] has shown that these elongated amorphous islands occur at the front and back peripheral regions next to the buried amorphous bands in both the temperature-independent and dependent regime of the critical dose for amorphization.

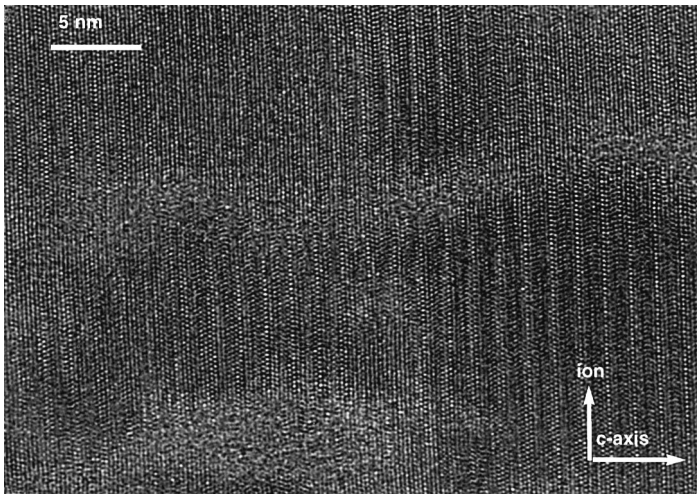

Fig. 2. HRTEM of the onset of amorphization in Si ion irradiated SiC.

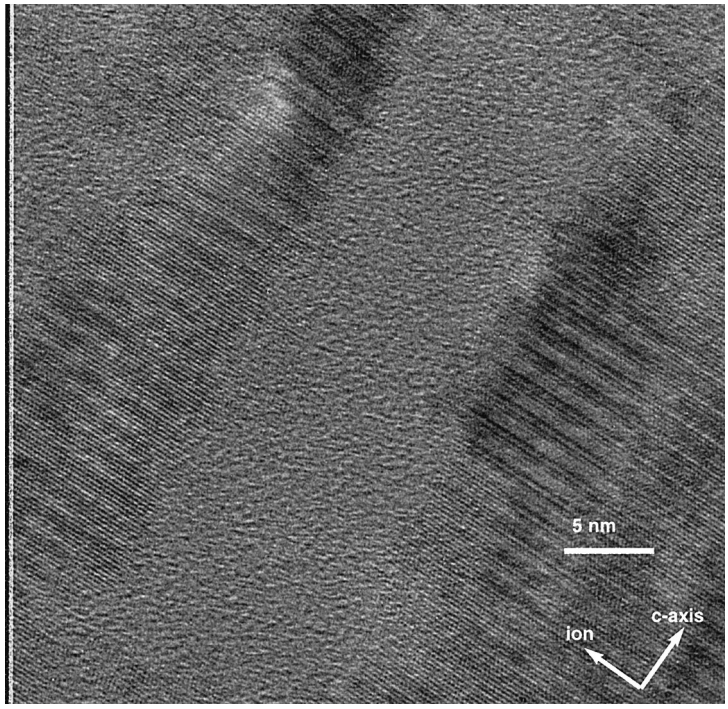

Fig. 3. HRTEM of the amorphous island structure for Si ion irradiated SiC.

The anisotropic geometry of these islands relative to the surface of the specimens raises the question of whether there is a strain effect on the evolution of the amorphous structure. There is obviously a large lattice strain induced in the crystal to amorphous transition both from point defect accumulation and the amorphous pockets. Also, the presence of the free surface should affect the

nature of the strain field. The obvious question from these results is whether the formation and connection of the amorphous pockets are being affected in a substantial way by this phenomenon. It is possible that the tensile stress in the crystalline regions adjacent to a buried amorphous (due to the associated volumetric expansion upon amorphization) could contribute to drive the surrounding material amorphous. The presence of the free surface would affect this strain field and possibly the amorphization threshold. In summary it is speculated that the critical threshold for amorphization, or the amorphization kinetics may be different in the in situ and ex situ techniques due to stress-dependent phenomenon.

3.2. Amorphization under neutron irradiation

Neutron irradiated specimens were studied using both TEM and X-ray diffraction analysis. Fig. 4 shows an electron diffraction pattern for the Cree 6H–SiC specimen that was irradiated in contact with the HFIR coolant water to a dose of ~2.56 dpa. Note that ~10°C temperature rise above the coolant water is assumed as the irradiation temperature. The diffraction pattern shown in Fig. 4 shows diffuse rings typical of amorphous material. There was no indication of diffraction spots anywhere in the sample and no contrast was found in dark field imaging. X-ray analysis (performed on the sample prior to sample thinning for TEM) showed no evidence of crystallinity.

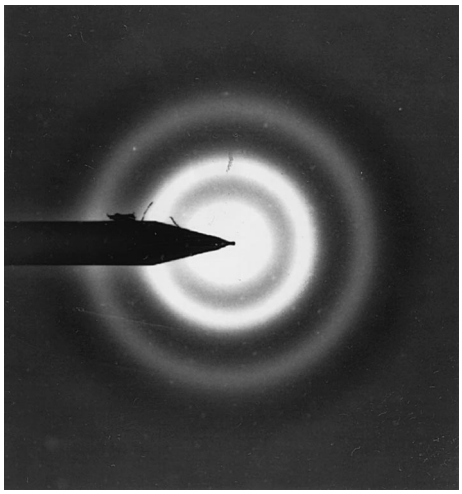

Fig. 4. Electron diffraction pattern of neutron amorphized SiC.

3.3. Density, hardness and elastic modulus of amorphous SiC

Mechanical properties such as density, elastic modulus and hardness of amorphized single crystal SiC have been previously estimated from measurements of surface or buried amorphous layers of ion beam irradiated material. Specifically, the density has been inferred by surface step height measurements [4,35,36] or by observing the increase in total range with TEM [7,30,37,38], yielding a density decrease ranging from about −22% to −15%. The residual hardness (H_{irr}/H_{unirr}) [30,35,36,39] and residual modulus (E_{irr}/E_{unirr}) [30,39] have likewise ranged in the literature from 45% to 70% (relative hardness) and 70–76% (relative modulus.)

The measurement of physical properties of neutron amorphized single crystal SiC has several advantages over the techniques required for ion implanted samples. Specifically, the neutron amorphized sample is a bulk sample as compared to a buried or surface amorphous layer previously used. The density can therefore be made using very accurate techniques such as the density gradient column used in this study. For the 2.56 dpa irradiated 6H–SiC the density was found to be 2.857 g/cc, or a 10.8% reduction in density from the 3.204 g/cc unirradiated value. The uncertainty in the measurement of density is approximately 0.001 g/cc. The Carborundum sintered α-SiC (Hexoloy) and Cercom hot pressed β-SiC irradiated in the target region of the High Flux Isotope Reactor had density changes of 11.1% and 10.1%, respectively. These values, as well as the amorphized single crystal values are substantially less than the density changes estimated in previous ion beam studies (i.e. a 15–22% reduction).

The bulk nature of the specimens also allows measurement of elastic modulus and hardness without concern for substrate effects. Using a Nanoindenter-II, as was used in some of the previous ion beam studies [4,30,37], the measured hardness of the neutron amorphized 6H–SiC decreased

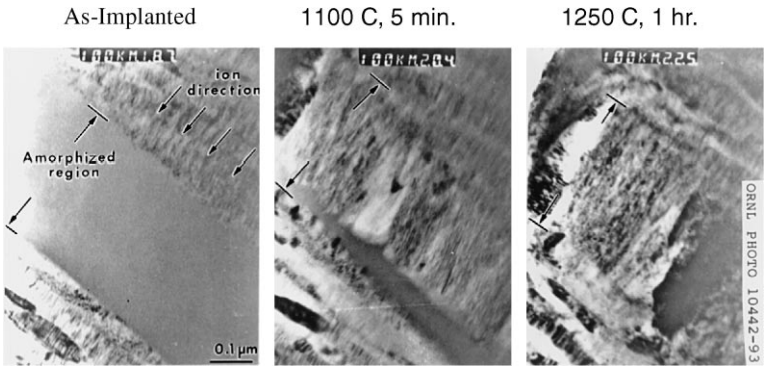

Fig. 5. Epitaxial growth of SiC in a buried carbon ion beam amorphized SiC layer.

from 38.7 ± 2 to 21.0 ± 1 GPa, while the elastic modulus decreased from 528 ± 14 to 292 ± 5 GPa. This corresponds to a residual hardness (H_{irr}/H_{unirr}) of 54 ± 4% which is in rough agreement with previous estimates. However, the 55 ± 2% residual modulus is significantly lower than previous estimates obtained on ion-irradiated specimens, which may be explained from sensing of the higher modulus substrate. Also of interest is that the hardness and modulus of CVD SiC amorphized by 3 MeV carbon ions, were measured with a Nanoindenter-I to be 32 and 275 GPa, respectively, on a cross-sectioned specimen (where crystalline substrate effects were minimized) [40].

3.4. Recrystallization of amorphous SiC

Several studies have been conducted over the past 20 years investigating the recrystallization of amorphized SiC [4,38,41] [42–48]. As has been pointed out by McHargue in a recent review articles on ion implantation effects in SiC, [4] the reported regrowth temperature for amorphous SiC covers a wide range from 750°C to 1700°C. Various techniques have been employed to study recrystallization including Raman spectroscopy, cross-sectional TEM and RBS.

Fig. 5 shows an example of epitaxial regrowth of SiC. In this figure a buried amorphous layer of SiC has been formed by 3.0 MeV carbon ions on CVD SiC. The as-implanted micrograph (left) shows about an ~0.35 μm buried amorphous layer of SiC. As the temperature was raised to 1100°C the apparent epitaxial regrowth of crystalline SiC was observed to occur at amorphous edge closest to the implanted surface, and within 5 min recrystallization of the amorphous layer was nearly complete. Following a 1250°C anneal for 1 h there was no evidence of amorphous material remaining.

An obvious question for all of the recrystallization studies performed on ion-irradiated SiC concerns the possible roles of the implanted ions and underlying crystalline material on the crystallization kinetics. The neutron irradiations are advan-

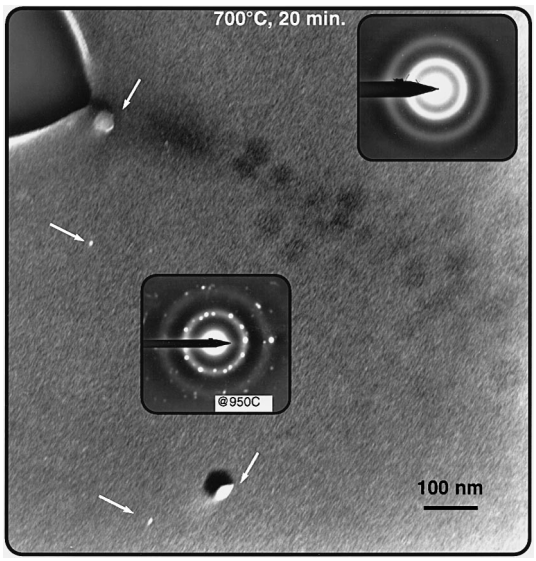

Fig. 6. Surface contamination-induced recrystallization of bulk amorphous SiC.

tageous for studying the recrystallization behavior of amorphous SiC both because it is a bulk material and because it is a relatively "clean," impurity free material. Fig. 6 shows the first sign of recrystallization in the in situ TEM annealing study for the neutron amorphized SiC. This figure gives a dark field image of the amorphous material with a few contrast points (indicated by white arrows) nucleating after several minutes at 700°C. Through-focus micrographs revealed them to be surface crystallites and by comparison with micrographs taken before the annealing began, were matched with surface irregularities attributed to contamination. As the temperature increased, these nucleating sites grew slowly, but they did not readily expand through the thickness of the TEM foil.

Fig. 7 shows a bright field image taken at 950°C in a thicker region of greater foil thickness as compared to Fig. 6. At temperatures above ~800°C crystallite growth occurred at widely spaced intervals between which large, completely amorphous areas remained. The nucleating crystal type has not been identified, though it is apparently highly twinned perpendicular to its growth direction. Observation of a limited number of these star shaped crystallites such as those shown in Fig. 7 were made as a function of annealing time and temperature. It was observed that the crystallites grew slowly in the ~800–1100°C temperature range and that the crystallite size as a function of annealing temperature was approximately linear. However, in the annealing step between 1125 and 1150°C, the recrystallization kinetics appeared much more rapid, with both faster growth of the existing crystallites and spontaneous nucleation throughout the amorphous material occurring. Fig. 8 shows micrographs at the beginning (~1 min) and ~7 min into the annealing at 1150°C. Note that the white arrow indicates the same crystallite in both micrographs. By comparing the two images, the new recrystallized sites which appeared between the existing crystallites are apparent. Following 30 min of annealing at 1150°C, no evidence of amorphous material was found in a detailed examination of the sample. The diffraction rings of this polycrystalline material were indexed to be beta SiC (fcc). These general findings corroborate the more recent studies on recrystallization on ion-im-

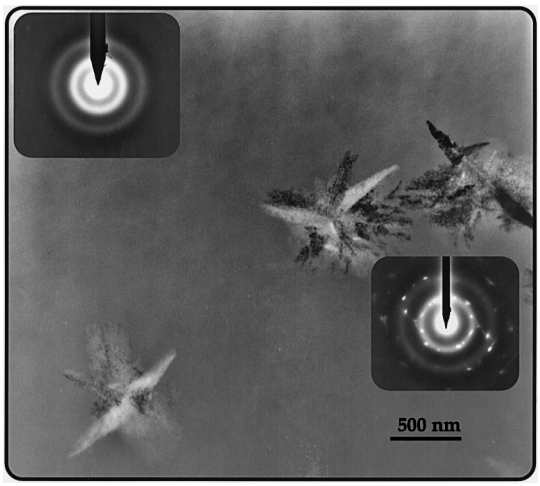

Fig. 7. Bulk nucleation and growth in amorphous SiC.

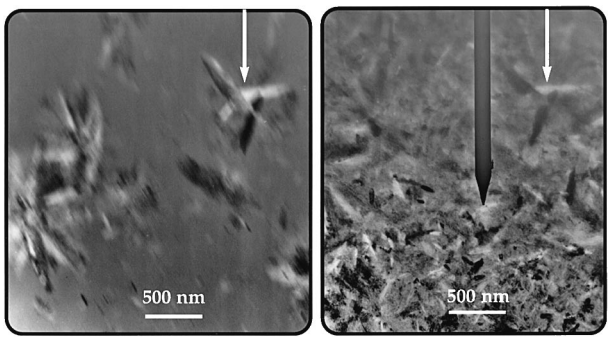

Fig. 8. Spontaneous nucleation and rapid growth in amorphous SiC at 1150°C.

planted specimens as reviewed by Heera [45], though are significantly different from many of the older references possibly due to suppression or acceleration of crystallite nucleation due to implanted ion effects. However, more study is required to rule out thin-film effects on the recrystallization temperature in the present in situ annealing study. It was seen in this study that the nucleating "star" crystallites began inside the thicker regions of the foil. This may be due to the higher probability of nucleating a crystal in the larger volume, but may also indicate that the foil surface is suppressing nucleation.

4. Conclusions

(1) A temperature dependent threshold for amorphization for implanted 0.56 MeV silicon ions of approximately 420 K exists, above which amorphization at 1×10^{-3} dpa/s will not occur. This falls roughly between the ~300 K threshold temperature for point-defect producing electron irradiation and the ~500 K threshold temperature for the heavily damaging xenon ions employed by previous researchers.

(2) The observation of elongated amorphous islands in the crystalline regions on both sides of the amorphous band for the silicon ion-implanted silicon carbide, which are independent of temperature and crystal orientation, suggests that a strain effect is compromising the calculation of threshold dose in bulk ion irradiated materials as well as in situ ion irradiation experiments.

(3) The first irrefutable demonstration of fast neutron induced amorphization in ceramic materials has been made. Specifically, at a fast neutron dose equivalent to 2.56 dpa amorphized single crystal α-SiC at an irradiating temperature and flux of ~70°C and 8×10^{-7} dpa/s, respectively.

(4) Measurements taken on bulk amorphous SiC have yielded accurate determination of material property changes occurring in the crystal to amorphous transition. Specifically, the measured properties for amorphized single crystal 6H SiC are: density = 2.857 g/cc (10.8% swelling), elastic modulus = 292 ± 5 GPa and hardness = 21.0 ± 1 GPa.

(5) Recrystallization studies of the neutron-irradiated high purity, amorphous SiC indicated that recrystallization occurs in three stages. At the low temperature stage, 700°C, nucleation of crystalline SiC occurs at surface contamination sites, though does not appear to grow rapidly into the bulk. At intermediate temperatures of ~800–1100°C, crystallites nucleate heterogeneously in the bulk amorphous SiC and grow slowly with increasing temperature. In the temperature range of 1125–1150°C spontaneous nucleation and rapid growth of new crystallites occur uniformly in the amorphous material. Following 30 min at 1150°C the material is completely crystalline.

(6) Crystalline hcp 6H α-SiC, which was amorphized under neutron irradiation, recrystallizes to highly faulted fcc β-SiC.

Acknowledgements

The authors would like to thank Marie Williams and Wade Jones for help in the preparation of the TEM specimens and Jim Bentley for useful discussions and assistance with the TEM. Research sponsored by the Office of Fusion Energy Sciences, US Department of Energy under contract DE-AC05-96OR22464 with Lockheed Martin Energy Research Corp.

References

[1] W. Primak, L.H. Fuchs, P.P. Day, Phys. Rev. 103 (1956) 1184.
[2] R. Blackstone, E.H. Voice, J. Nucl. Mater. 39 (1971) 319.
[3] C.W. White et al., Mater. Sci. Rep. 4 (1989) 41.
[4] C.J. McHargue, J.M. Williams, Nucl. Instr. and Meth. B 80/81 (1993) 889.
[5] W.J. Weber, L.M. Wang, N. Yu, Nucl. Instr. and Meth. B 116 (1996) 322.
[6] L.L. Snead, D. Steiner, S.J. Zinkle, J. Nucl. Mat. 191–194 (1992) 566.
[7] L.L. Snead, S.J. Zinkle, in: I.M. Robertson, et al. (Eds.), MRS Symposium on Microstructure of Irradiated Materials, Boston, MA., vol. 373, Materials Research Society, Inc., 1995, p. 595.
[8] D.P. White, J. Appl. Phys. 73 (1993) 2254.
[9] R.R. Hart, H.L. Dunlap, O.J. Marsh, Radiat. Eff. 9 (1971) 261.

[10] J.M. Williams, C.J. McHargue, B.R. Appleton, Nucl. Instr. and Meth. 209/210 (1983) 317.
[11] J.A. Spitznagel et al., Nucl. Instr. and Meth. B 16 (1986) 237.
[12] J.A. Edmond, R.F. Davis, S.P. Withrow, K.L. More, J. Mater. Res. 3 (1988) 321.
[13] N.G. Chechenin et al., Nucl. Instr. and Meth. B 65 (1992) 341.
[14] L.L. Horton et al., Nucl. Instr. and Meth. B 65 (1992) 345.
[15] C. Kinoshita et al., Proceedings of the 11th International Conference on Electron Microscopy, Japanese Society of Electron Microscopy, 1986.
[16] H. Inui, H. Mori, T. Sakata, Phil. Mag. B 66 (1992) 737.
[17] H. Inui, H. Mori, H. Fujita, Phil. Mag. B 61 (1990) 107.
[18] A. Matsunaga, C. Kinoshita, K. Nakai, Y. Tomokiyo, J. Nucl. Mater. 179–181 (1991) 457.
[19] S.D. Harrison, J.C. Corelli, J. Nucl. Mater. 99 (1981) 203.
[20] R.A. Wullaert et al., in: J.F. Kircher, R.E. Bowman (Eds.), Effects of Radiation on Materials and Components, Reinhold, New York, 1964, p. 277.
[21] E. Lell, N.J. Kreidl, J.R. Hensler, in: J.E. Burke (Ed.), Progress in Ceramic Science, vol. 4, Pergamon Press, Oxford, 1966, p. 1.
[22] F.W. Clinard, Jr., L.W. Hobbs, in: R.A. Johnson, A.N. Orlov (Eds.), Physics of Radiation Effects in Crystals, Elsevier, Amsterdam, 1986, p. 387.
[23] T. Tanabe, S. Muto, K. Niwase, J. Nucl. Mater. 175 (1989) 258.
[24] K. Niwase, K. Nakamura, T. Shikama, T. Tanabe, J. Nucl. Mater. 170 (1990) 106.
[25] B.T. Kelly, J. Nucl. Mater. 172 (1990) 237.
[26] H. Inui, Phil. Mag. B 65 (1992) 1.
[27] W.J. Weber, R.C. Ewing, L.M. Wang, J. Mater. Res. 9 (1994) 688.
[28] W.J. Weber, L.M. Wang, Nucl. Instr. and Meth. B 106 (1995) 298.
[29] W.J. Weber, N. Yu, Proceedings of the International Conference on Defects in Insulating Materials, 1996, accepted.
[30] W.J. Weber, N. Yu, L.M. Wang, N.J. Hess, J. Nucl. Mater. 244 (1997) 258.
[31] S.J. Zinkle, L.L. Snead, Nucl. Instr. and Meth. B 116 (1996) 92.
[32] J.F. Ziegler, J.P. Biersack, U. Littmark, The Stopping and Range of Ions in Solids, Pergamon Press, New York, 1985.
[33] A.T. Motta, D.R. Olander, Acta Metall. Mater. 38 (1990) 2175.
[34] H. Inui, H. Mori, H. Fujita, Acta Metall. 37 (1989) 1337.
[35] C.J. McHargue et al., Mat. Sci. Eng. 69 (1985) 123.
[36] C.J. McHargue, C.S. Yust, J. Am. Ceram. Soc. 67 (1984) 117.
[37] L.L. Snead, S.J. Zinkle, in: I.M. Robertson et al. (Eds.), Microstructure Evolution During Irradiation, MRS Symposium Proceedings, vol. 439, Materials Research Society, Pittsburgh, 1997, p. 595.
[38] J. Bentley, L.J. Romana, L.L. Horton, C.J. McHargue, in: G.S. Was, L.E. Rehn, D.M. Follstaedt (Eds.), Phase Formation and Modification by Beam-Solid Interactions, Materials Research Soc., 1992, p. 363.
[39] C.J. McHargue, D.L. Joslin, J.M. Williams, Nucl. Instr. and Meth. B 46 (1990) 185.
[40] L.L. Snead, S.J. Zinkle, D. Steiner, J. Nucl. Mat. 191–194 (1992) 560.
[41] R.B. Wright, D.M. Gruen, Radiat. Eff. 33 (1977) 133.
[42] B.R. Appleton et al., Nucl. Instr. and Meth. B 1 (1984) 167.
[43] P.S. Sklad, P. Angelini, C.J. McHargue, J.M. Williams, in: G.W. Bailey (Ed.), Proceedings of the 42nd Annual Mtg. Electron Micro. Soc. Amer., San Franscisco Press, San Franscisco, Ca, 1984, p. 416.
[44] H.G. Bohn, J.M. Williams, C.J. McHargue, G.M. Begun, J. Mater. Res. 2 (1987) 107.
[45] V. Heera, J. Stoemenos, R. Kogler, W. Skorupa, J. Appl. Phys. 77 (1995) 2999.
[46] J. Heindl et al., Inst. Phys. Conf. Ser. 146 (1995) 435.
[47] V. Heera, R. Kogler, W. Skorupa, J. Stoemenos, Appl. Phys. Lett. 67 (1995) 1999.
[48] K. Yoshii et al., Thin Solid Films 199 (1991) 85.